

# Ultimate Shear Tests of Prestressed Concrete I-Beams Under Concentrated Loading

By Shunji Inomata\*

## 1. Introduction

When a prestressed concrete beam is subjected to an ultimate strength test, the behavior of the member may be described with reference to the uncracked and cracked range. In the uncracked range the response to load is approximately linear. However, at cracking a fundamental change takes place in the way in which the beam resists load. Two important cases should be considered. When flexure action predominates, the strain distribution remains linear up to the point of failure in case of bonded tendons. But, when shear is significant, inclined cracks develop, and in the region of inclined cracking the strain distribution becomes non-linear. If shear is critical, the inclined cracking leads to a shear failure.

The flexure failure mechanism had been elucidated. The shear failure mechanism has been studied extensively, both in reinforced and prestressed concrete<sup>1)-11)</sup>. Very often conclusions are too limited to be sufficiently valid to define design criteria which will satisfy the overall problem embracing all types of beams and all conditions of loading.

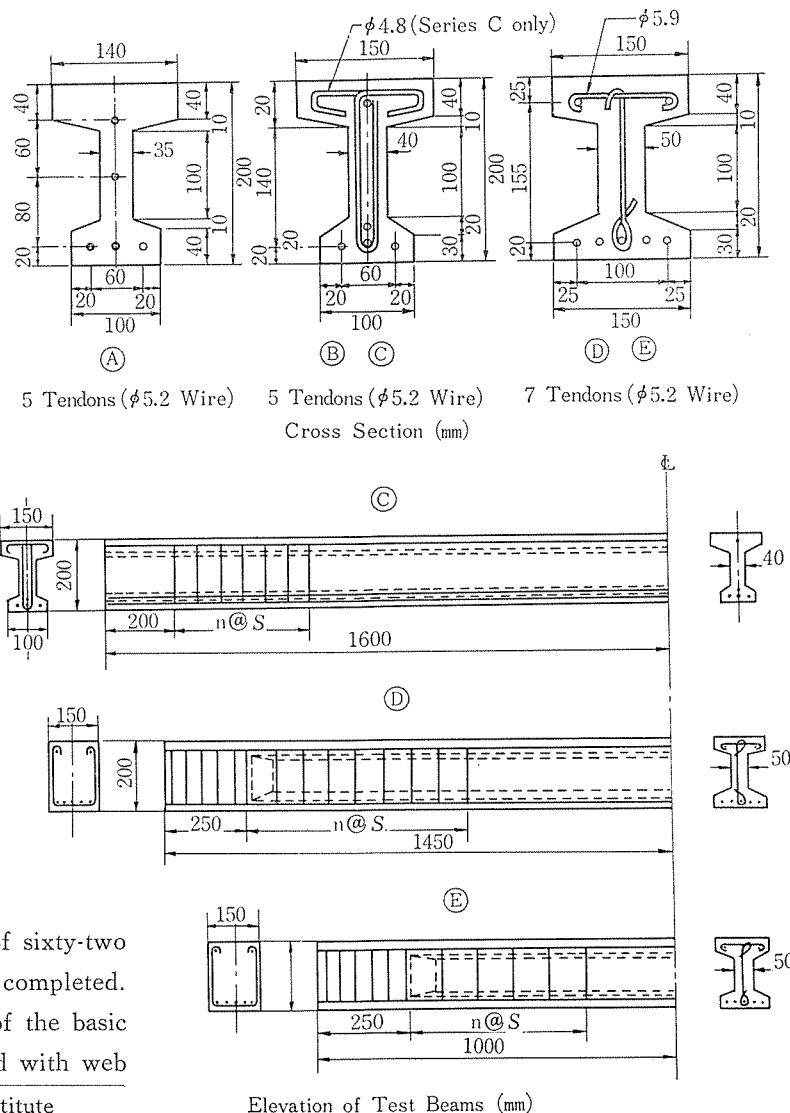
A study of the overload behavior of sixty-two pretensioned prestressed I-beams was completed. This work led to an investigation of the basic shear strength of I-beams without and with web

reinforcement. Only the principal results of these tests are presented herein. In addition, the test results are compared to the provisions of ACI 318-63.

## 2. Test Specimens

Elevations and cross sections of the test beams,

Fig. 1 (a) Test Beams



\* Dr. Eng. Japan Bridge & Structural Institute

Fig. 1 (b) Test Beams (Web Reinforcement)

Series	Beam No.	$S$ (cm)	$n$	$nS$ (cm)
C	1, 2	6.0	7	42
	3	12.0	4	48
	4	18.0	3	54
	5, 6	8.0	8	64
	7	13.0	5	65
	8	18.0	4	72
	9	10.0	9	90
	10, 11	14.0	6	84
	12	18.0	5	90
	13	14.0	8	112
	14, 15	16.0	7	112
	16	18.0	6	108
D	3, 4	11.0	9	99
	7, 8	8.0	13	104
	11, 12	6.0	17	102
E	1, 2	8.0	8	64
	3, 4	12.0	5	60
	5, 6	16.0	4	64
	7, 8	18.0	3	54

referred to as A, B, C, D and E Series, are shown in Fig. 1. In case of A, B and C Series lengths of shear span were changed to inspect the effects of shear span to height ratio on the shear failure of I-beam without web reinforcement. In D Series, the effects of the prestressing force on the shear failure were investigated and in E Series the effects of a moving load were verified on the beams having different amount of web reinforcement.

Table 1 shows the calculated prestress in each series beam assuming that creep factor  $\phi$ , amount of shrinkage  $\epsilon_s$ , and relaxation of prestressing steel are equal to 2.0,  $20 \times 10^{-5}$  and 5 percent, respectively.

All the beams were manufactured by pre-tensioning process. Prestress was slowly transferred to the test beams on the fourth or fifth day after casting, after which the specimens were stored in

Table 1 Calculated Prestress (kg/cm<sup>2</sup>)

Series	Beam No.	Initial Tensioning Stress of Tendon	Effective Prestress	
			Top	Bottom
A	No. 1~No. 15	10 600	+ 9	+120
B	No. 2~No. 12	11 900	- 3	+146
C	Nn. 1~No. 16	11 900	- 3	+146
D	No. 1~No. 4	11 370	+16	+126
	No. 5~No. 8	5 640	+60	+ 60
	No. 9~No. 12	950	- 1	+ 5
E	No. 1~No. 9	11 370	+16	+126

the laboratory until the time of testing.

Compression tests were conducted on concrete cylinders to determine the compressive strength of the concrete associated with the test beams at the time of prestress transfer and at the time of test. Splitting tests on concrete cylinders were also carried out to determine the tensile strength of the concrete. The results of these tests are presented in Table 2. The values are an average of three or more tests.

Table 2 Properties of the Concrete (kg/cm<sup>2</sup>)

Series	Beam No.	At Transfer		At Test		
		Age (days)	Compressive Strength	Age (days)	Compressive Strength	Tensile Strength
A	No. 1~No. 6	4	341	140	462	
	No. 9~No. 9	4	343	136	480	
	No.10~No. 12	4	336	125	483	
	No.13~No. 15	4	326	120	473	
B	No. 2~No. 4	4	316	149	489	39
	No. 5~No. 8	5	327	137	456	39
	No. 9~No. 12	5	336	132	460	40
C	No. 1~No. 4	5	333	141	477	39
	No. 5~No. 8	5	319	133	473	44
	No. 9~No. 12	5	334	129	455	39
	No.13~No. 16	5	333	123	478	39
D	No. 1~No. 4	4	355	120	435	
	No. 5~No. 8	4	363	115	453	
	No. 9~No. 9	4	370	110	455	
E	No. 1~No. 3	4	352	120	446	38
	No. 4~No. 6	4	348	120	428	39
	No. 7~No. 9	4	364	120	433	39

Table 3 shows the characteristics of the steel employed in this test.

In order to improve bond strength of wire, special deformed prestressing wire was used. This

Fig. 2 Load-Strain Curves for Steel

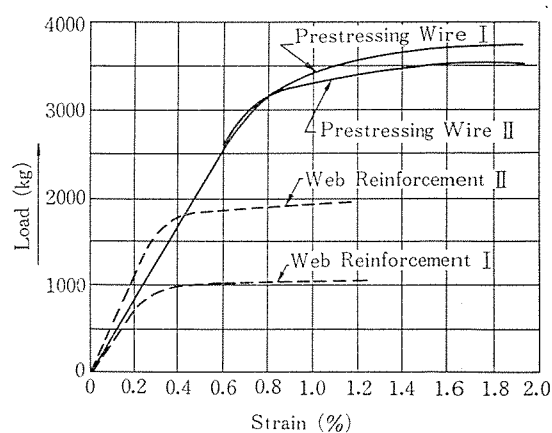


Table 3 Characteristics of the Steel

	Prestressing Steel		Web Reinforcement		
	I	II	I	II	
Cross-sectional area	22.7	21.1	18.1	27.3	mm
Proportional limit (0.02%)	125	143	47.5	61.6	kg/mm <sup>2</sup>
Proof limit (0.2%)	153	157	54.0	69.6	kg/mm <sup>2</sup>
Tensile strength	176	176	58.5	73.0	kg/mm <sup>2</sup>
Used in Series	A, B, C	D, E	C	D, E	

wire was manufactured by cold roll process and has the evenly projected deformations on its surface. Stress-strain curves for the steel used are shown in Fig. 2.

### 3. Procedure and Results

Loading tests were carried out applying one concentrated load or two symmetrical point loads on simply supported beams. In every test the distance between each end of the beam and the nearest support was more than 20 cm to avoid the support being within the region of the transmission length of the tendon employed.

The development of cracks, especially inclined cracking, was carefully observed.

#### (1) Series A

No web reinforcement was provided for the beams, as shown in Fig. 1. Shear failures were observed in this series on the beams tested on shear span ( $a$ ) to height of beam ( $h$ ) ratios varying from zero to five. The distances between two concentrated loads were 50 cm and 40 cm for the

Table 4 Test Results of Series A

Beam No.	$a/h$	Span Length	Load ( $\tau$ )	
		(cm)	Inclined Crack	Ultimate
1	0	50	24.5	41.2
2			22.4	34.7
3			22.7	30.1
4	0.3	62	17.5	30.0
5			15.0	21.7
6	0.6	74	14.6	21.7
7			13.0	14.5
8	1.5	110	6.7	11.0
9	2.0	130	5.0	7.5
10	2.5	150	4.8	6.3
11	3.0	170	4.7	5.0
12	4.0	200	3.7	3.9
13	5.0	200	3.2	4.0
14			3.4	4.0
15			3.6	3.9

beams No. 1~No. 11 ( $a/h=0\sim3.0$ ) and No. 12 ( $a/h=4.0$ ), respectively. One concentrated load was applied at the midpoint of the span length of the beams No. 13~No. 15 ( $a/h=5.0$ ).

The test results are shown in Table 4.

In case of the beams having the ratios less than 0.3, a vertical crack occurred in the middle part of the web at the support section and developed vertically in both directions with increased load. Under ultimate load the crush of the concrete was observed on the web or upper flange at the support section. Horizontal crack along the tendon situated in the web was also observed between the support and the nearest end of the beam.

For the beams having the  $a/h$  ratio less than 2.5 and greater than 0.6, the inclined cracks occurred in the web resulting in crushing the web concrete with a little increase of load after inclined cracking. These inclined cracks appeared suddenly on the line connecting the support and the loading point in the regions of the test beam where were as yet uncracked. In some instances only a single diagonal tension crack would form, however, more often two cracks would form almost simultaneously for the beam having greater the  $a/h$  ratio.

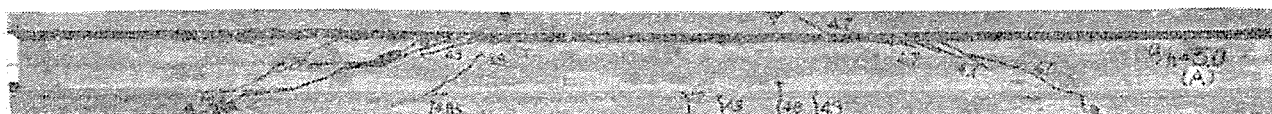
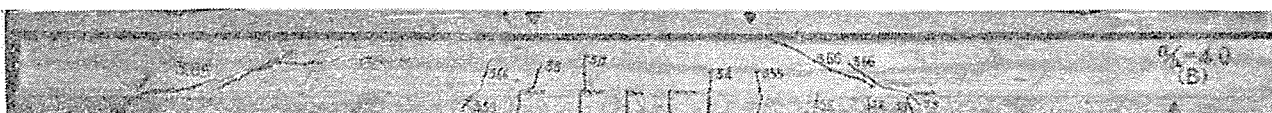
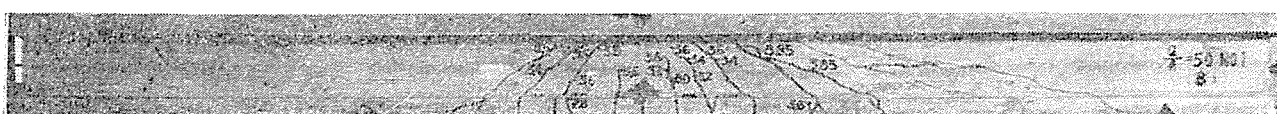
For the test beams having the  $a/h$  ratio greater than 4.0 flexural cracks occurred in the region of higher moment but, because of the presence of shearing forces, these cracks turned and inclined in the direction of increasing moment. The diagonal tension cracking would first appear, directly above the flexure crack and would quite often be followed by the development of adjacent diagonal tension cracking in the test beams with the  $a/h$  ratio 5.0. Under maximum load the crush of the web concrete would be observed.

Typical developments of the cracks after failure are shown in Fig. 3.

#### (2) Series B

Span lengths of the test beams were 200 cm for beam No. 2~No. 4 and 280 cm for beam No. 5~No. 11, respectively. All the beams were not

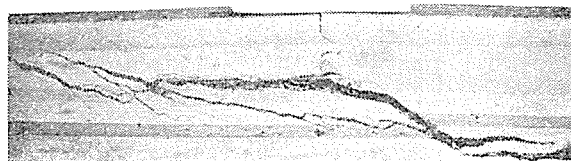
Fig. 3 Test Beams after Failure (Series A)

No. 1 ( $a/h=0$ )No. 5 ( $a/h=0.6$ )No. 8 ( $a/h=1.5$ )No. 10 ( $a/h=2.5$ )No. 11 ( $a/h=3.0$ )No. 12 ( $a/h=4.0$ )No. 13 ( $a/h=5.0$ )

Close-up of Crushed Web

No. 10 ( $a/h=2.5$ )

Tension Cracks in Top Flange

No. 15 ( $a/h=5.0$ )

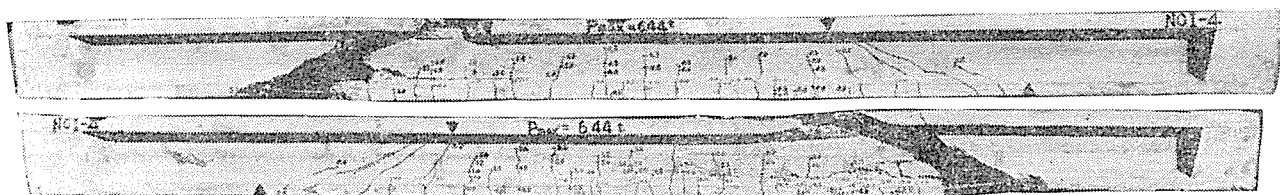
provided with web reinforcement. Test results are indicated in Table 5.

Two or more diagonal tension cracks would form in the region of shear span after flexure cracks would be observed in the region of higher bending, except beams No. 2 and No. 3. For most of the test beams with the  $a/h$  ratio greater than 3.0, the inclined cracking which finally was associated with failure was diagonal tension cracking which appeared to be precipitated by the

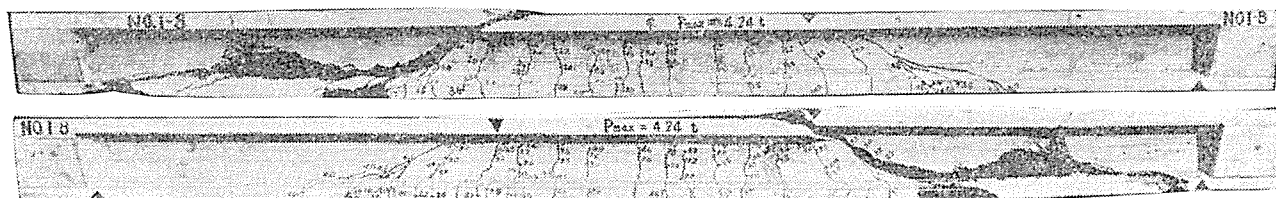
Table 5 Test Results of Series B

Beam No.	$a/h$	Load (t)	
		Inclined Crack	Ultimate
2	1.5	7.52	12.14
3	2.0	6.03	9.51
4	2.5	5.44	6.44
5	3.0	5.74	6.19
6	4.0	4.34	4.89
7	5.0	3.24	3.49
8		3.34	4.24
9	6.0	2.92	3.24
10		2.80	3.06
11	7.0	2.62	3.12
12		2.74	2.88

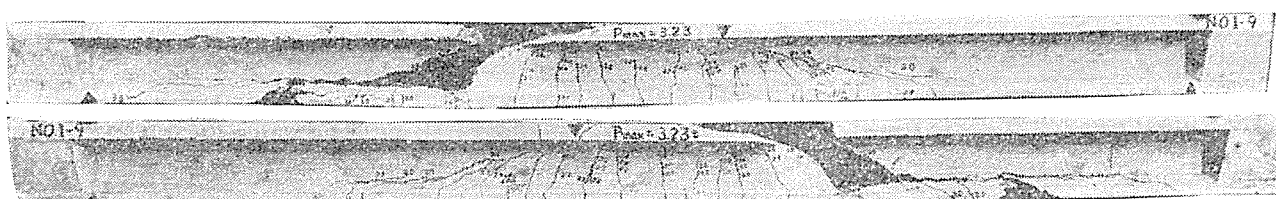
Fig. 4 Test Beams after Failure (Series B)



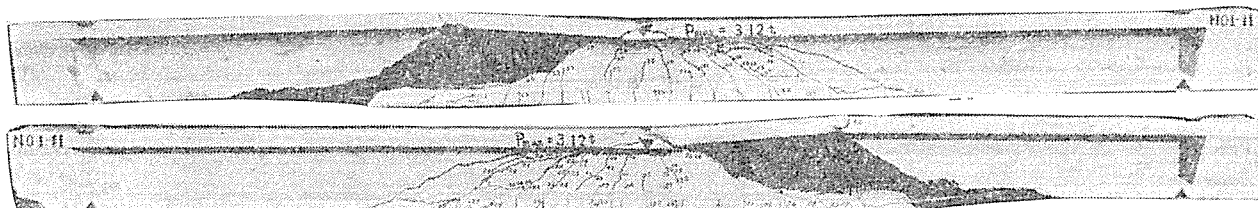
No. 4 ( $a/h=2.5$ )



No. 8 ( $a/h=5.0$ )



No. 9 ( $a/h=6.0$ )

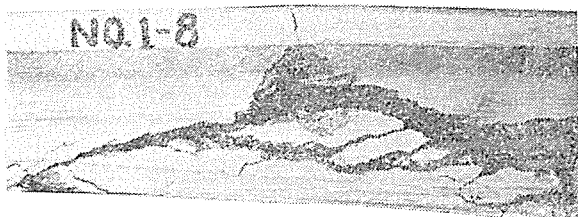


No. 11 ( $a/h=7.0$ )

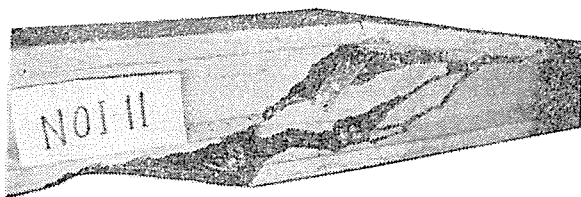
Close-up of Crushed Web



No. 6 ( $a/h=4.0$ )

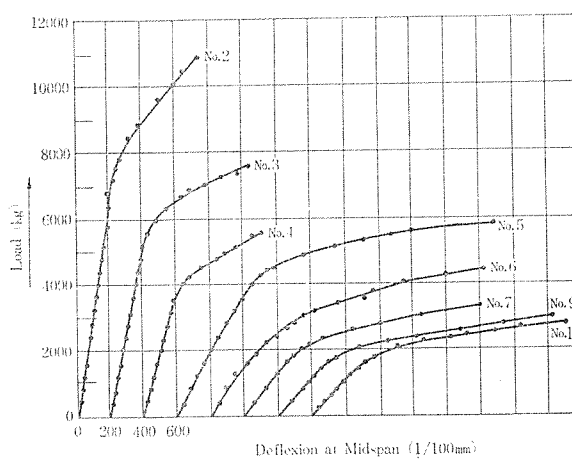


No. 8 ( $a/h=5.0$ )



No. 11 ( $a/h=7.0$ )

Fig. 5 Load-Deflection Curves (Series B)



initial formation of flexure crack. The diagonal tension cracking would first appear directly above the flexure crack and be followed by the development of adjacent diagonal tension cracking while still at the same shear. In most instances with higher  $a/h$  ratio the failure developed from this

inclined crack initially forming at a horizontal distance from the load point greater than twice the total depth of the test beam. The failures generally appeared to start near the intersection of an inclined crack in the web and the top flange of the beam. Tension cracks in the top flange were evident in every case after failure.

Typical formations of the cracks after failure are shown in **Fig. 4.** and load deflexion curves are indicated in **Fig. 5.**

### (3) Series C

In this series the principal variables were the amount of web reinforcement as shown in **Fig. 1** and the shear span to total depth ratio.

All the test beams having 280 cm span length were subjected to two symmetrical point loads.

The test results are indicated in **Table 6.**

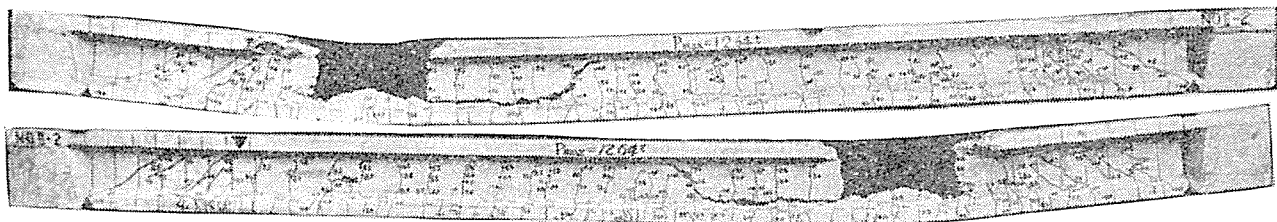
So far as the development of inclined crack was concerned, no difference was observed between the test beams with and without web reinforcement. Almost all the test beams failed in bending following the crush of the top flange concrete.

**Table 6 Test Results of Series C**

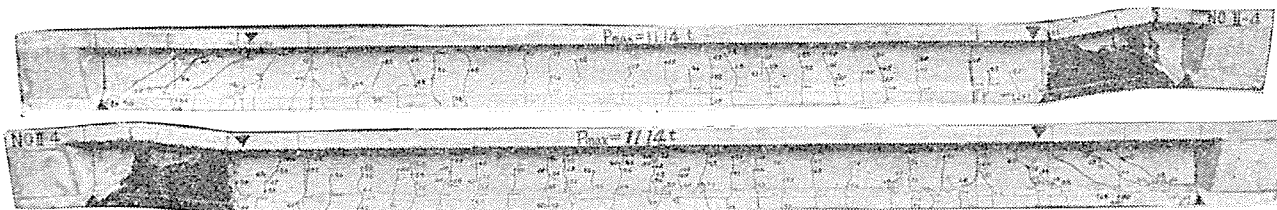
Beam No.	$a/h$	Spacing of Web Reinforcement (cm)	Load (t)	
			Inclined Crack	Ultimate
1	2.0	6.0	5.74	13.02
2		6.0	5.84	12.64
3		12.0	5.94	10.51
4		18.0	4.54	11.14
5	3.0	8.0	5.68	8.86
6		8.0	4.74	8.32
7		13.0	4.38	6.92
8		18.0	4.84	7.76
9	4.0	10.0	3.88	6.04
10		14.0	3.54	6.08
11		14.0	3.71	5.86
12		18.0	3.14	6.00
13	5.0	14.0	2.76	4.62
14		16.0	2.72	4.65
15		16.0	3.34	4.80
16		18.0	2.92	5.05

But in the beams No. 3 and No. 7 the lower end of an inclined crack extended into the low flange of the beam and the complete disintegration of the low flange was observed in the region of shear span. For the beam No. 8, crushing of the top flange concrete occurred in shear span showing shear-compression type failure under

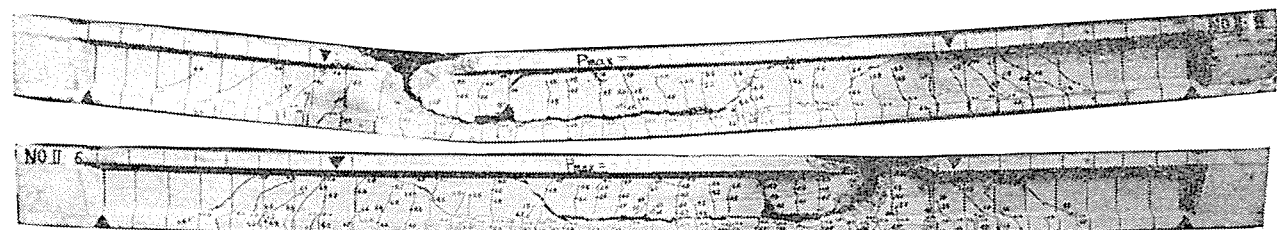
**Fig. 6 Test Beams after Failure (Series C)**



No. 2 ( $a/h=2.0$ ,  $S=6.0$  cm)



No. 4 ( $a/h=2.0$ ,  $S=18.0$  cm)



No. 6 ( $a/h=3.0$ ,  $S=8.0$  cm)



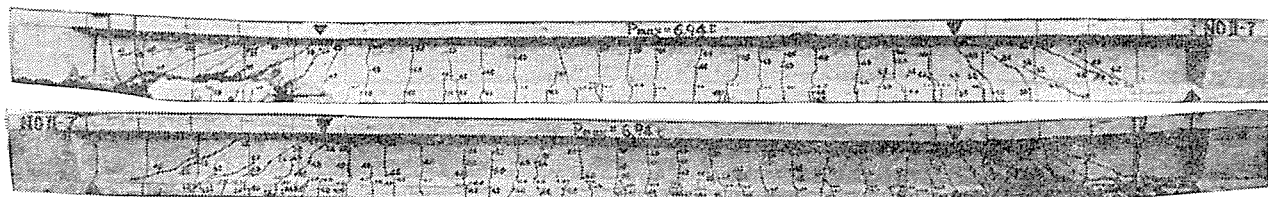
the ultimate load.

Typical development of the cracks after failure

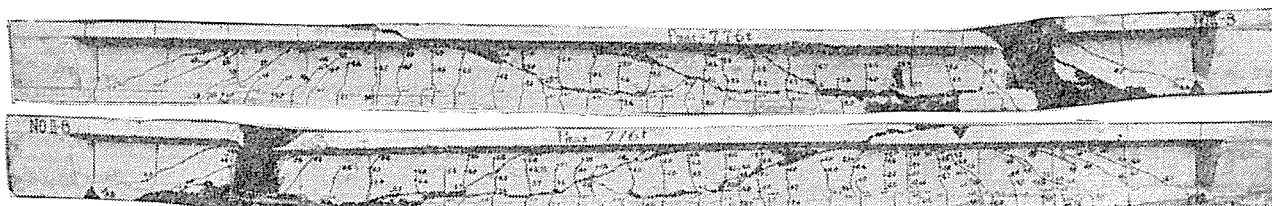
and load-deflexion curves are shown in **Fig. 6** and

**Fig. 7**, respectively.

**Fig. 6** (Continued)



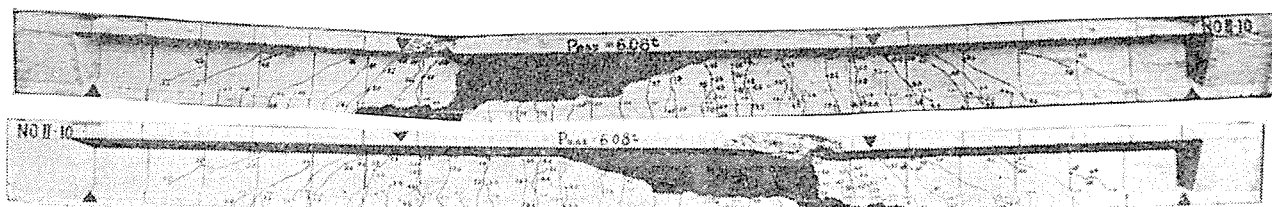
No. 7 ( $a/h=3.0$ ,  $S=13.0$  cm)



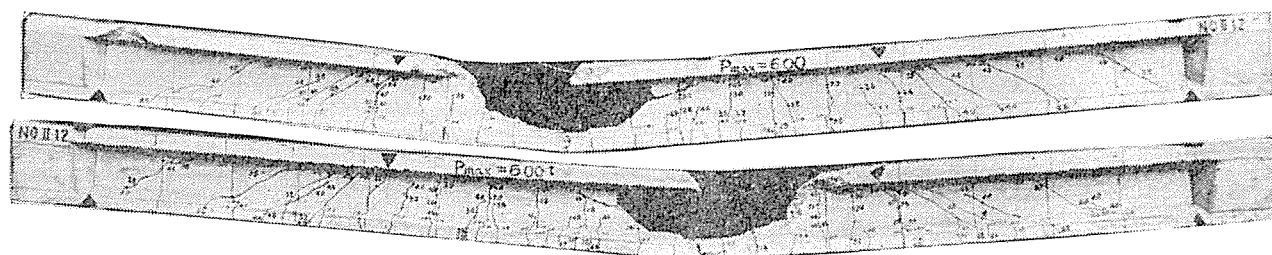
No. 8 ( $a/h=3.0$ ,  $S=18.0$  cm)



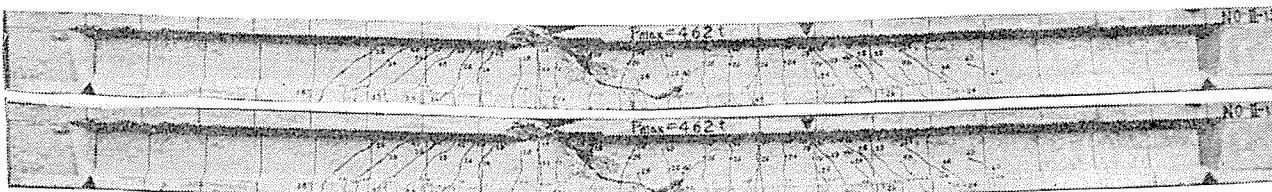
No. 9 ( $a/h=4.0$ ,  $S=10.0$  cm)



No. 10 ( $a/h=4.0$ ,  $S=14.0$  cm)



No. 12 ( $a/h=4.0$ ,  $S=18.0$  cm)



No. 13 ( $a/h=5.0$ ,  $S=14.0$  cm)

Fig. 6 (Continued)

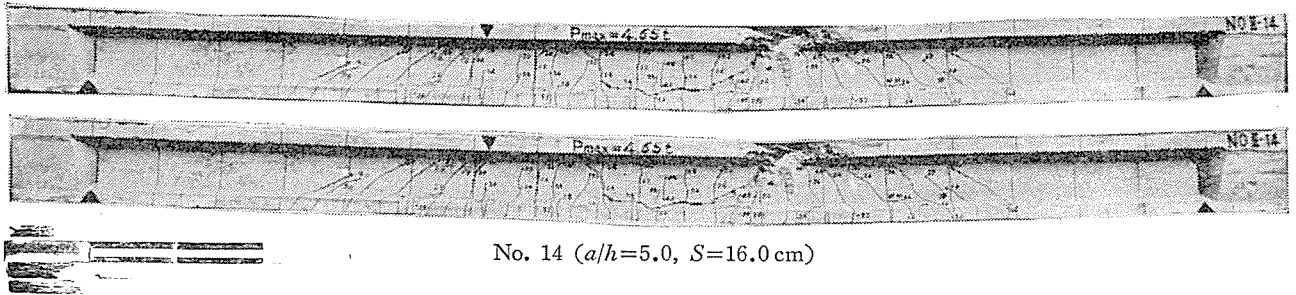
No. 14 ( $a/h=5.0$ ,  $S=16.0$  cm)

Fig. 7 Load-Deflection Curves (Series C)

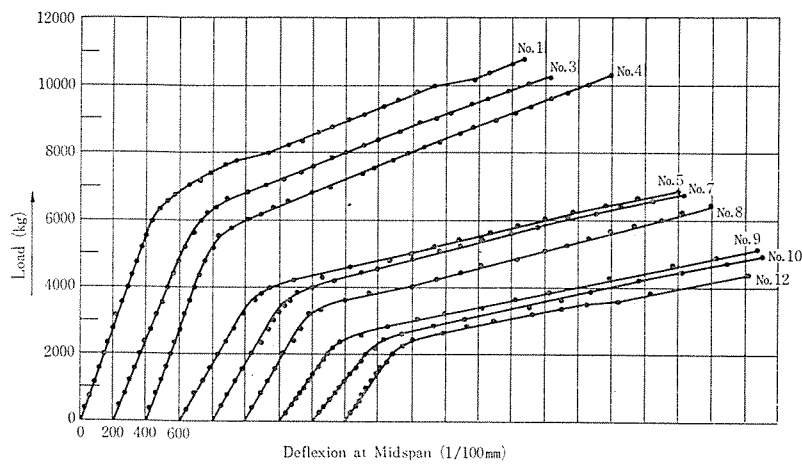


Table 7 Test Results of Series D

Beam No.	Web Reinforcement Spacing $s$ (cm)	Initial Prestressing Force (t)	Load (t)		
			Flexure Crack	Inclined Crack	Ultimate
1	Non	16.8	3.38	4.50	5.12
2	Non		3.10	4.60	4.68
3	$s=11.0$		3.20	4.60	6.36
4	$s=11.0$		3.40	4.80	6.54
5	Non	8.4	2.44	3.20	4.52
6	Non		2.35	3.20	5.05
7	$s=8.0$		2.20	3.20	6.32
8	$s=8.0$		2.15	3.00	6.35
9	Non	1.4	1.16	2.20	3.11
10	Non		1.12	2.00	2.53
11	$s=6.0$		1.14	2.20	6.17
12	$s=6.0$		0.98	2.40	5.83

## (4) Series D

In this series the principal variables were the amount of web reinforcement and of prestress.

All the test beams of 240 cm span length were subjected to two point loads having a constant  $a/h$  ratio of 4.5.

The test results are indicated in Table 7.

A shear compression failure occurred in the test beam without web reinforcement at ultimate load. The lower end of an outmost inclined crack would extend horizontally into the lower flange of the beam and the separation between the web and the lower flange would be observed.

All the test beams with web reinforcement failed in bending resulting in the crushing of the concrete in the top flange of the region where the moment was maximum.

Typical crack patterns and load deflection curves are indicated in Fig. 8 and Fig. 9.

## (5) Series E

The span length (150 cm) of each beam was divided into equal six parts, designated as point A, B, C, D, E, F and G as shown in Fig. 10.

One concentrated load was applied in increasing load increments of 4000 kg up to a previously

Fig. 8 Test Beams after Failure (Series D)

No. 1  $P_i=16.8$  t (Without Web Reinforcement)No. 3 ( $P_i=16.8$  t,  $S=11.0$  cm)



Fig. 8 (Continued)

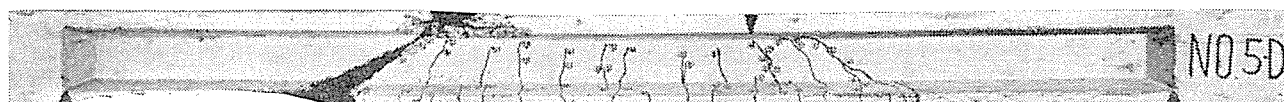
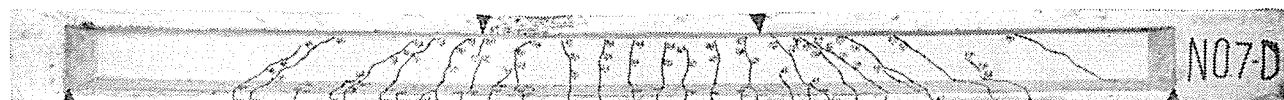
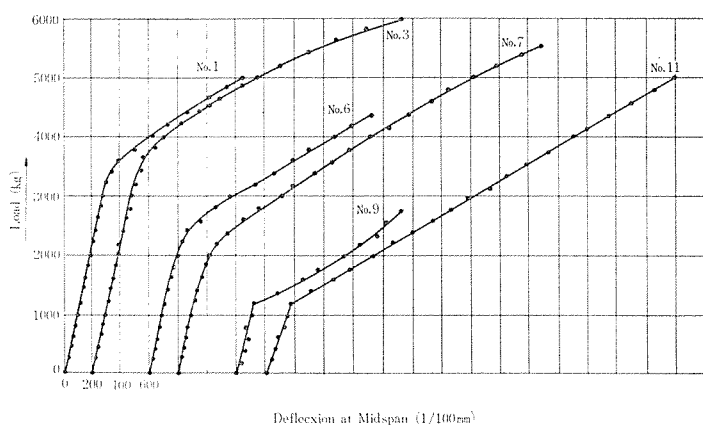
No. 5  $P_i=8.4$  t (Without Web Reinforcement)No. 7  $P_i=8.4$  t,  $S=8.0$  cmNo. 10  $P_i=1.4$  t (Without Web Reinforcement)No. 11  $P_i=1.4$  t,  $S=6.0$  cmNo. 12  $P_i=1.4$  t,  $S=6.0$  cm

Fig. 9 Load-Deflection Curves (Series D)

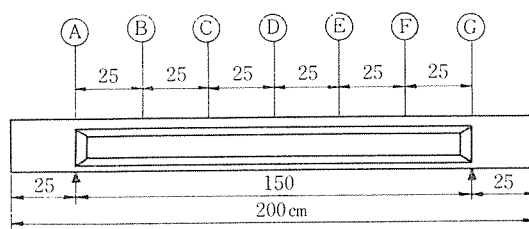


fixed value and then was reduced to zero. After having finished this loading and unloading, the load was moved to the next loading position. Moving the load from point A to point G and coming back from point G to point A, the same loading process was repeated at each position. This loading procession was referred to one complete cycle of

Table 8

Maximum Load	
Cycle	Max. Load (t)
First	3.2
Second	4.0
Third	4.8
Fourth	5.6
Fifth	6.4
Sixth	7.2
Seventh	8.0
Eighth	8.8

Fig. 10 Loading Points (Series E)



loading on the test beam. After finishing one cycle of loading, the maximum load to be applied was increased by 800 kg and the same loading process was repeated. The maximum load of each loading cycle is

indicated in Table 8.

The test results are shown in Table 9.

All the test beams failed in bending except beams No. 3 and No. 6 which failed in shear compression.

Typical crack patterns are shown in Fig. 11.

(6) Observed modes of shear failure on the test beams without web reinforcement.

In the beams tested, inclined cracks occurred in two different ways, which were discussed by several authors in their literatures.

In beams with high prestress and short shear

Table 9 Test Results of Series E

Beam No.	Spacing of Web Reinforcement (cm)	Load (t)*	
		Initial Flexure Cracking	Ultimate
1	8.0	4.80 (3-C)	8.10 (8-D)
2		4.80 (3-E)	8.01 (8-D)
3	12.0	4.60 (3-C)	7.30 (7-E)
4		4.40 (3-D)	8.00 (8-D)
5	16.0	4.40 (3-C)	8.03 (8-D)
6		4.60 (3-E)	7.31 (8-D)
7	18.0	4.40 (3-D)	7.20 (6-C)
8		4.60 (3-D)	7.15 (6-E)

\* Figures in parenthesis show the order of loading cycle and the loading position when as initial flexure crack is observed or failure of the test beam occurs.

spans the principal tensile stresses in the web may exceed the tensile strength of the concrete before flexure cracks occur in the shear span. An inclined crack which occurs in the web before flexure cracks appear is referred to as a web-shear crack.

In beams with moderate prestress and relatively long shear spans, flexure cracks will occur in the shear span before the principal tensile stresses in the web are high enough to cause web-shear cracks. If an inclined crack does occur in such a beam, it is either the extension of a flexure crack in the shear span or it occurs over or beside such a flexure crack. This type of inclined crack is referred to as a flexure-shear crack, since

Fig. 11 Tests Beams after Failure (Series E)

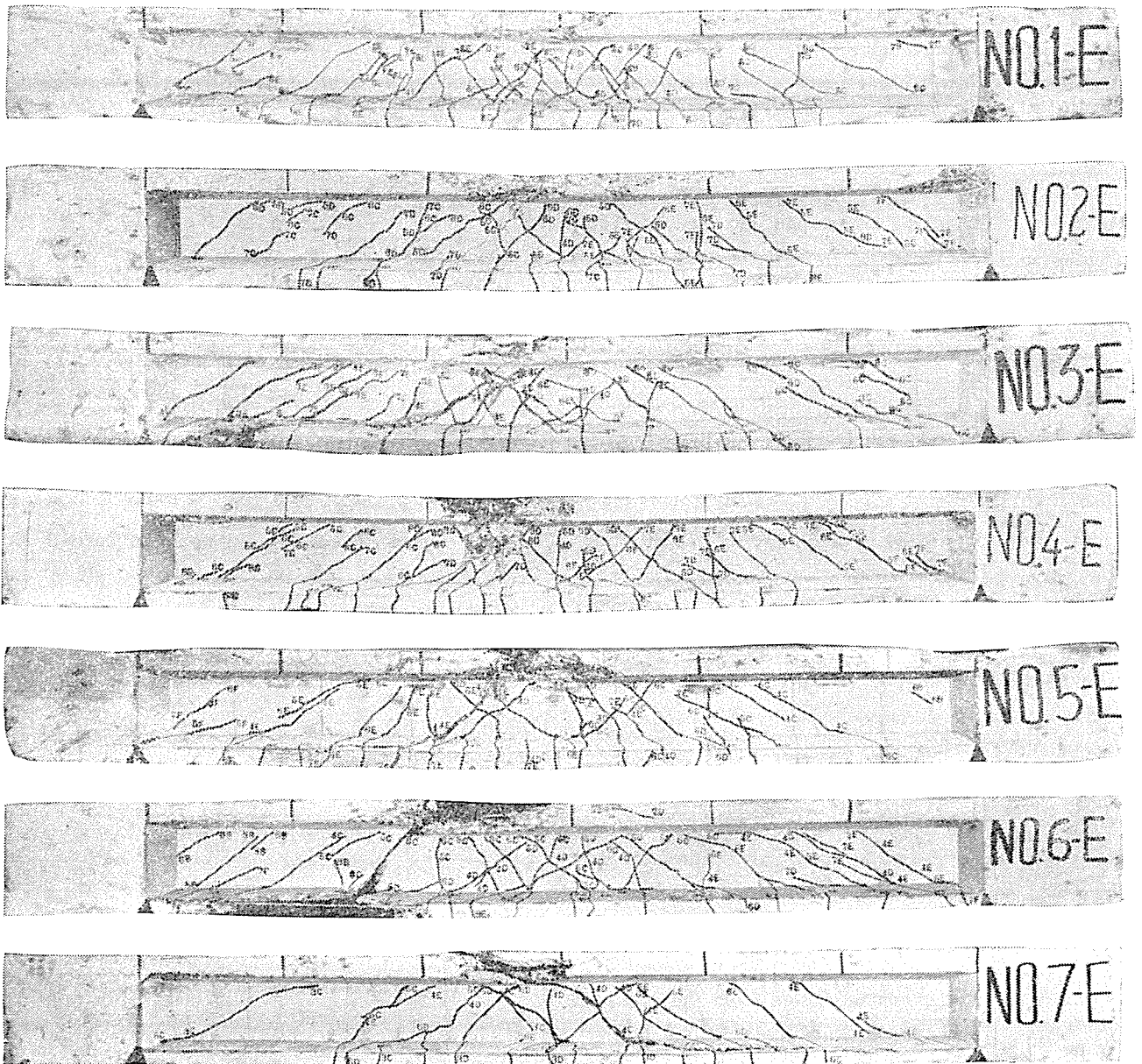
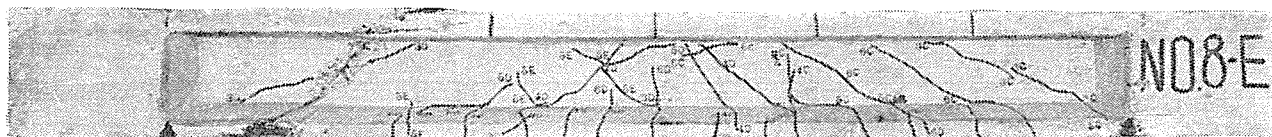
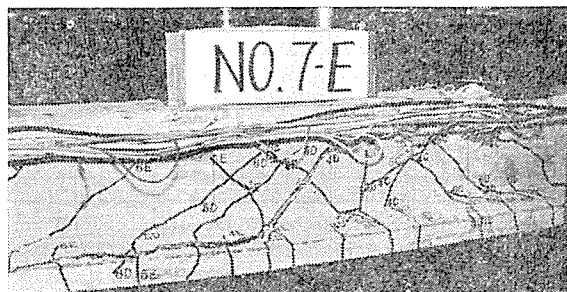


Fig. 11 (Continued)



Close-up of Web Cracks



the flexure cracks in the shear span contribute to the development of the inclined crack, is referred to as an initiating crack.

**Beams with web-shear cracks** The actual mechanism of failure in shear depended on the type of inclined cracks which had developed in the beam. A web-shear crack causes a redistribution of the stresses in the shear span and beam action ceases and the beam carries load as a tied arch. The compression thrust line over the inclined crack is generally close to the crack and almost parallel to it. Hence, the thrust acts with a considerable eccentricity on the portion of the beam over the crack near the reactions. This was evidenced by tension cracks in the top flange as illustrated by beam No. 10 in Series A. These cracks were followed immediately by crushing of the web.

**Beams with flexure-shear cracks** After a flexure-shear crack develops, the linear relationship between concrete and steel strains ceases to exist since the concrete strains are concentrated above the end of the inclined crack while the steel strains are distributed over a length at least equal to the horizontal projection of the crack. When the concrete strains reach a limiting value, crushing occurs, destroying the beam. This type of failure is known as a shear-compression failure.

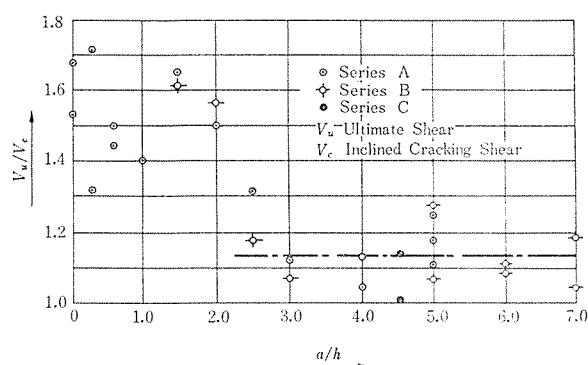
If the prestressing steel becomes unbonded by separation of the tension flange from the rest of the beam, this may constitute the primary failure before a shear-compression failure occurs.

In a number of beams, the inclined crack and the splitting along the prestressing steel shortened the anchorage zone so much that a secondary failure occurred in the tendon anchorages. This occurred after the inclined cracks had formed and the inclined cracking load was not affected by the failure of the anchorage bond.

### 3. Discussion

#### (1) Strength of test beams without web reinforcement

The ultimate load for the beams without web reinforcement was either equal to or only slightly less than the inclined cracking load in case of relatively large value of shear span to height ratio as shown in **Fig. 12**. For  $a/h > 2.0$  the test beams can carry some additional load beyond inclined cracking but the increase is about 13 percent on the average, therefore it may safely be said that the useful capacity of the beam corresponds to the inclined cracking load. For  $a/h$

Fig. 12 Relation between  $V_u/V_c$  ratio and  $a/h$ 

<2.0 relatively large increase in the load can be observed but the scatter in the magnitude is also large. This could be attributed to the local strengthening effects caused by load and reaction concentrations.

In the case of web-shear cracking, and only in this case, the principal tensile stresses computed for an uncracked section will approximate the stresses in the web of the beam at the time of inclined cracking.

For biaxially stressed concrete subjected to combined compressive and tensile stresses a simple criterion can be used expressing in the form,

$$\frac{\sigma_1}{f_t} + \frac{\sigma_2}{f_c} = 1 \dots\dots\dots (1)$$

where  $f_c$  and  $f_t$  represent the uniaxial compression and tensile strengths respectively. This equation gives an acceptable representation of the envelope in the compression-tension zone for plane state of stress. The principal stresses are converted into the normal and shear stresses.

$$\left. \begin{aligned} \sigma_1 &= \sqrt{\left(\frac{\sigma_x - \sigma_y}{2}\right)^2 + \tau^2} - \frac{\sigma_x + \sigma_y}{2} \\ \sigma_2 &= \sqrt{\left(\frac{\sigma_x - \sigma_y}{2}\right)^2 + \tau^2} + \frac{\sigma_x + \sigma_y}{2} \end{aligned} \right\} \dots\dots\dots (2)$$

Then Eq. (1) gives

$$\begin{aligned} (f_c + f_t) \sqrt{\left(\frac{\sigma_x - \sigma_y}{2}\right)^2 + \tau^2} \\ - (f_c - f_t) \left(\frac{\sigma_x + \sigma_y}{2}\right) &= f_c f_t \\ \tau^2 &= \frac{f_c f_t}{(f_c + f_t)^2} \{f_c - (\sigma_x + \sigma_y)\} \\ &\quad \{f_t + (\sigma_x + \sigma_y)\} + \sigma_x \sigma_y \dots\dots\dots (3) \end{aligned}$$

or,

$$\begin{aligned} \left(\frac{\tau}{f_c}\right)^2 &= \frac{f_c f_t}{(f_c + f_t)^2} \left\{1 - \left(\frac{\sigma_x + \sigma_y}{f_c}\right)\right\} \\ &\quad \left\{\frac{f_t}{f_c} + \left(\frac{\sigma_x + \sigma_y}{f_c}\right)\right\} + \left(\frac{\sigma_x}{f_c}\right) \left(\frac{\sigma_y}{f_c}\right) \dots\dots\dots (3a) \end{aligned}$$

The strength of the concrete in pure tension may be derived from the compressive strength by the following simple formula.

$$f_t = 7 + 0.06 f_c \dots\dots\dots (4)$$

Eq. (4) gives the following values.

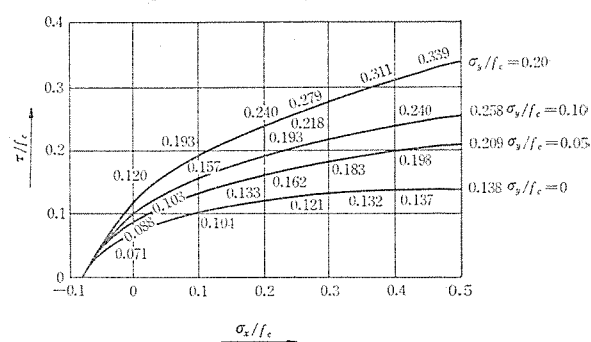
$f_c$ (kg/cm <sup>2</sup> )	$f_t$ (kg/cm <sup>2</sup> )	$f_t/f_c$	$f_t f_c / (f_t + f_c)^2$
350	28	0.080	0.0686
400	31	0.077	0.0668
450	34	0.075	0.0653
500	37	0.074	0.0640
Mean.....		0.076	0.066

In the range of the compressive strength being considered, the values of  $(f_t/f_c)$  and  $f_c f_t / (f_c + f_t)^2$  seem to be constant. Using those mean values, Eq. (3a) can be written as follow;

$$\begin{aligned} \left(\frac{\tau}{f_c}\right)^2 &= 0.06 \left\{1 - \left(\frac{\sigma_x + \sigma_y}{f_c}\right)\right\} \\ &\quad \left\{0.076 + \left(\frac{\sigma_x + \sigma_y}{f_c}\right)\right\} + \left(\frac{\sigma_x}{f_c}\right) \left(\frac{\sigma_y}{f_c}\right) \dots\dots\dots (3b) \end{aligned}$$

The relations between  $\sigma_x/f_c$ ,  $\sigma_y/f_c$  and  $\tau/f_c$  are shown in Fig. 13. If it is assumed that the critical shear stress in the web can be determined as shown in Fig. 13 then it should be possible to compute the web-shear cracking load.

Fig. 13 Envelope for Failure



The constantly changing combinations of shearing stress and flexure stress and near the loads and reactions, bearing stress, make it difficult to determine the location and magnitude of the maximum principal tensile stress in a beam at the time of inclined cracking. Thus the inclined crack may originate at, above, or below the elastic centroid, and anywhere along the length of the shear span where the stresses are large enough. It could be assumed that in beams with short shear spans and thin webs, the maximum principal tensile stress along the potential inclined crack occurs at the centroid. As the shear span gets longer or the web thickness increases, flexure stresses have a greater effect on the magnitude of the principal tensile stresses and the point of maximum stress tends to move toward the tension flange. At the same time, however, the properties of the beam become such that flexure cracks develop in the shear span before inclined cracking, and the computed stresses in the uncracked web cease to have any significance. Thus, in beams similar to those tested, it can be assumed that the web-shear cracking load can be determined by

considering only the principal tensile stresses at the elastic centroid of the uncracked section.

The shearing stress at the centroid under web-shear cracking shear  $V_{cw}$  can be computed by the following elastic formula.

$$\tau_{cw} = \frac{V_{cw} Q_g}{b_0 I}$$

$$V_{cw} = b_0 \frac{I}{Q_g} \tau_{cw} \dots \dots \dots (5)$$

where  $Q_g$  = statical moment of the cross-sectional area above (or below) that level about the centroidal axis

$\tau_{cw}$  = critical shear stress

There must, however, be one important reservation, in calculating the principal tensile stresses account has to be taken of the compressive stresses acting on the horizontal planes near the points of application of loads and reactions. By using the data from theoretical studies and also the results of deformation test on beams, the effect of  $\sigma_y$  could be neglected in case of higher  $a/h$  ratio than 2.0. It is generally difficult to estimate the exact distribution of the vertical stress,  $\sigma_y$ , and some part of the applied load will be transmitted directly to the nearest support by a strut being formed in the web. Considering the above-mentioned facts, the effective shearing force of which should be taken account in the calculation of shearing stress  $\tau$  could be assumed to be  $\mathcal{H}V$ . This reduction factor  $\mathcal{H}$  could be given as follow;

$$\mathcal{H} = \frac{1}{2} \left( \frac{a}{h} \right) \leq 1.0 \dots \dots \dots (6)$$

Therefore web-shear cracking shear  $V_{cw}$  is given by the following formula.

$$V_{cw} = \frac{1}{\mathcal{H}} b_0 \frac{I}{Q_g} \tau_{cw} \dots \dots \dots (7)$$

Table 10 Calculated Web-shear (Cracking Shear)

Series	Compressive Strength (kg/cm <sup>2</sup> )		Effective Prestress (kg/cm <sup>2</sup> )	$\tau_{cw}$ (kg/cm <sup>2</sup> )	$I/Q_g$ (cm)	$V_{cw}$ ( t )			
	$f_{cm}$	$f_{ck}$	$\sigma_x$			$a/h$			
						$\geq 2.0$	1.5	1.0	0.6
A	476	437	60	48	14.9	2.50	3.33	5.00	8.33
B	465	427	63	48	14.9	2.86	3.81	5.72	9.53
C	471	432	63	48	14.9	2.86	3.81	5.72	9.53
D	435	399	70	47	15.0	3.53	4.71	7.06	11.76
	453	416	34	41	15.0	3.07	4.09	6.14	10.23
	475	436	3	32	15.0	2.40	3.20	4.80	8.00
E	436	400	70	47	15.0	3.53	4.71	7.06	11.76

In applying the above formulas, the characteristic compressive strength  $f_{ck}$  of the concrete is defined by the following relations, adopting the 5% probability level.

$$f_{ck} = f_{cm}(1 - 1.64 \delta)$$

$\delta$  = dispersion coefficient = 5%

The calculated web-shear cracking shear is given in Table 10.

An inclined crack which develops after flexural cracks have formed in its vicinity in the shear span is defined as a flexure-shear crack. Tests show, however, that cracking under bending and shear is extremely complex and that the so-called flexure-shear crack can only be indentified when it forms and develops clearly and independently of other cracking. But this happens only in short shear spans. In large shear spans and on the less prestressed beams it is difficult to ascertain the stage at which an existing crack transforms itself into a potential failure crack. In such cases considerable cracking will precede formation of the fatal diagonal crack. The difficulty of precise recognition and identification of the potential flexure-shear cracking stage is accentuated by the fact that it is practically impossible to predict accurately the location of the flexure-shear crack and the accompanying mode of failure.

Various attempts have been made to express this flexure-shear cracking phenomenon in terms of a rational theory based on the ordinary theory of flexure, but they have not yield any solution of general applicability; from conventional reinforced concrete to fully prestressed concrete.

It is assumed, in this paper, that an inclined crack starts from a point where axial concrete strain attains  $f_t/E_c$  at the flexural cracking section.

The analysis for the cracking moment is carried out by adopting the following assumptions (Fig. 14 (a)).

- (1) The tensile strain of the concrete is limited to the maximum value of 2.5 times the elastic tensile strain  $f_t/E_c$ .
- (2) The tensile stress dia-



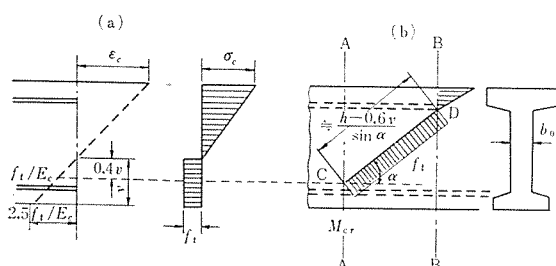
gram of the concrete can be replaced by a rectangular diagram determined by the value of the constant tensile stress  $f_t$  and its depth is taken to be equal the zone subjected to elongation.

(3) The stress diagram in the compressive zone is a triangular diagram and the stresses are calculated with the same modulus  $E_c$ .

**Table 11** Calculated Flexure-shear Cracking Shear  
(Beams without web reinforcement)

Series	Beam No.	$a/h$	$f_t$ (kg/cm <sup>2</sup> )	$v$ (cm)	$M_{cr}$ (t-cm)	$f_t b_0 (h-0.6v)^2$ (t-cm)	$M_{ci}$ (t-cm)	$V_{ci}$ (t)
A	11	3						2.35
	12	4	33	6.4	111	30	141	1.76
	13, 14, 15	5						1.41
B	5	3						2.90
	6	4						2.18
	7, 8	5	33	6.4	141	33	174	1.74
	9, 10	6						1.45
	11, 12	7						1.24
D	1, 2		31	5.6	164	43	207	2.30
	5, 6	4.5	32	7.7	105	38	143	1.59
	9, 10		33	10.9	54	30	84	0.94

**Fig. 14** Analysis for Cracking State



An inclined crack is assumed to initiate from point C at the cracking section A-A and have an inclination  $\alpha$  (Fig. 14 (b)). Just before a formation of this inclined crack CD, the constant tensile stress  $f_t$  is likely to act normally to this diagonal section. Considering the facts that the length of the diagonal section is nearly equal to  $(h-0.6v)/\sin \alpha$  and the effect of tensile force acting on the part of the upper flange upon the moment about the centroid of the compressive force at section B-B can be neglected due to its short lever arm, the bending moment at section B-B can be obtained as follow.

$$M_B = M_{cr} + \frac{b_0 f_t}{2} \frac{(h-0.6v)^2}{\sin \alpha} \dots \dots \dots (8)$$

The inclination  $\alpha$  depends upon the shear span lengths, the magnitude of prestress and the mode of loading, but the value of  $\alpha$  is assumed to be 45 degrees in this paper. Therefore initiating cracking moment  $M_{ci}$  and the corresponding shear can be obtained by the following relations.

$$M_{ci} = M_{cr} + f_t b_0 (h-0.6v)^2 \dots \dots \dots (9)$$

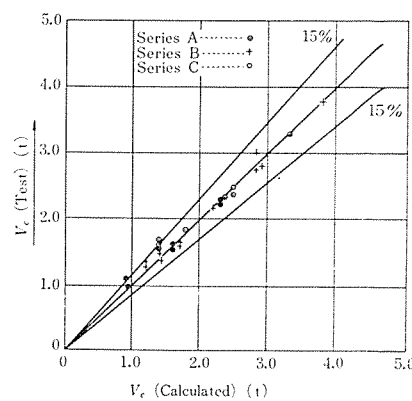
$$V_{ci} = M_{ci}/a \dots \dots \dots (10)$$

The calculated flexure-shear cracking shear  $V_{ci}$  is given in Table 11.

The calculated shears ( $V_{cw}$ ,  $V_{ci}$ ), plotted in Fig. 15 for the beams without web reinforcement for which  $a/h \geq 5$ , have a good correlation with the test values.

So far as the inclined cracking shear,  $V_{cw}$  or  $V_{ci}$ , is concerned, the provision of ACI 318-63 is always on the safe side giving 10 to 15% smaller inclined cracking shear than the observed ones and does not apply to the beams for which  $a/h \leq 2.0$ . There is no continuous gradation of the applicability of this provision from conventional reinforced concrete to fully prestressed concrete. In the case of the beams No. 9 and No. 10 of Series D, the observed flexure-shear cracking develops under a shear about 45% over the calculated value by the provision.

**Fig. 15** Comparison of Author's Equation with Test Evidence

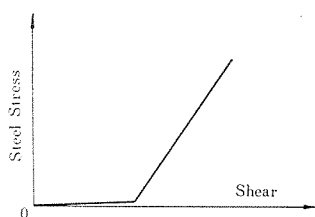


## (2) Strength of test beams with web reinforcement

The web reinforcement provides a means of transferring shear force across the crack and tends to restrain rotation at the cracked section. In ad-

dition, the development of splitting along the tension reinforcement is restrained, preventing failures due to the separation of the wires from the beam. The fact that the web reinforcement only becomes effective after the formation of an inclined crack acrossing the web reinforcement (**Fig. 16**) is widely recognized<sup>12)</sup>. And it is also reported that the observed increment of the steel stress has almost the same value calculated by the classical truss theory. Therefore the amount of web reinforcement required to prevent shear failure in a beam with straight wires can be assumed to be proportional to the difference between the inclined cracking load and the flexural failure load as shown in the following equation.

**Fig. 16 Relation between Shear & Steel Stress in Reinforcement**



$$V_u - V_c = V_s \quad \text{.....(11)}$$

where  $V_u$ =ultimate shear capacity of the section

$V_c$ =shear at inclined cracking load

$V_s$ =shear carried by the web reinforcement

Assuming that the horizontal projection of an inclined crack is equal to the effective depth of the beam the shear which is carried by the web reinforcement can be expressed in the following equation.

$$V_s = \frac{A_v f_{sg}}{S} d \quad \text{.....(12)}$$

where  $A_v$ =cross-sectional area of one stirrup

$f_{sg}$ =yield strength of the steel used

$S$ =spacing of stirrups

From those equations (11) and (12), the ultimate shear capacity of the section is given as follow.

$$V_u = V_c + \frac{A_v f_{sg}}{S} d \quad \text{.....(13)}$$

**Table 12 Calculated Ultimate Shear Capacity**

Series	Beam No.	$a/h$	$S$ (cm)	$A_v f_{sg} d/s$ (t)	$V_c$ (t)	$V_u$ (t)	$V_u^{B*}$ (t)
C	1, 2	2.0	6	4.31	2.86	7.17	5.76
	3		12	2.15	2.86	5.01	
	4		18	1.44	2.86	4.30	
	5, 6	3.0	8	3.23	2.86	6.09	3.84
	7		13	1.99	2.86	4.85	
	8		18	1.44	2.86	4.30	
	9	4.0	10	2.58	2.18	4.76	2.88
	10, 11		14	1.84	2.18	4.02	
	12		18	1.44	2.18	3.62	
	13	5.0	14	1.84	1.74	3.58	2.30
	14, 15		16	1.61	1.74	3.35	
	16		18	1.44	1.74	3.18	
	D	4.5	11	1.77	2.30	4.07	3.09
	7, 8		8	2.43	1.59	4.02	
	11, 12		6	3.24	0.94	4.18	

\*  $V_u^B$ : Ultimate shear corresponding to the calculated flexural failure load

**Table 13 Comparison between Calculated Shear and Observed Shear at Failure**

Series	Beam No.	Shear at Failure (t)		$\frac{V_{test}}{V_{cal.}}$	Mode of Failure
		Vcal.	Vtest		
C	1	5.74	6.51	1.13	Flexure
	2	5.74	6.32	1.10	Flexure
	3	5.01	5.26	—	Bond Failure
	4	4.30	5.57	1.30	Crush of Web
	5	3.84	4.43	1.15	Flexure
	6	3.84	4.16	1.08	Flexure
	7	3.84	3.47	—	Bond Failure
	8	3.84	3.88	1.01	Flexure
	9	2.88	3.02	1.05	Flexure
	10	2.88	3.04	1.06	Flexure
	11	2.88	2.93	1.02	Flexure
	12	2.88	3.00	1.04	Flexure
	13	2.30	2.31	1.00	Flexure
	14	2.30	2.33	1.01	Flexure
	15	2.30	2.40	1.04	Flexure
	16	2.30	2.52	1.10	Flexure
D	3	3.09	3.18	1.03	Flexure
	4	3.09	3.27	1.06	Flexure
	7	3.12	3.16	1.01	Flexure
	8	3.12	3.18	1.02	Flexure
	11	3.14	3.09	0.99	Flexure
	12	3.14	2.92	0.93	Flexure

Equation (13) coincides with that given by ACI 318-63.

The ultimate shear capacity, as shown in **Table 12**, is calculated by equation (13) for each beam of Series C and D. The steel stress  $f_{sg}$  is limited, in this calculation, to 4000 kg/cm<sup>2</sup> because of uncretain effectiveness of the end anchorage of stirrup.

These calculated values show that the ultimate shear capacity of the section is always greater than that is necessary to bring about the flexural failure, expect the beams No. 3 and No. 4 of Series C. The calculated shear is compared with the observed shear in Table 13.

Each beam for which the calculated shear capacity is greater than the shear to produce the flexural failure, is capable of withstanding safely the calculated flexural failure load.

### (3) Strength of test beams subjected to a moving load (Series E)<sup>13)</sup>

Shearing force at which an inclined crack occurs is calculated as shown in Table 14.

Ultimate shear capacity of the section is shown in Table 15.

Table 14 Web-shear or Flexure-shear Cracking Shear

$a$ (cm)	$V_{cw}$ (t)	$V_{ci}$ (t)	Inclined Cracking Shear (t)
25	5.65	8.29	5.65
50	3.53	4.14	3.53
75	3.53	2.76	2.76
100	3.53	2.07	2.07
125	3.53	1.66	1.66

Table 15 Calculated Ultimate Shear Capacity

$V_u(t)$ $S(cm)$	$V_c + A_v f_{sy} d/s$ (t)			
	8	12	16	18
25	8.00	7.29	6.87	6.74
50	5.98	5.17	4.75	4.62
75	5.21	4.40	3.98	3.85
100	4.52	3.71	3.29	3.16
125	4.11	3.30	2.88	2.75

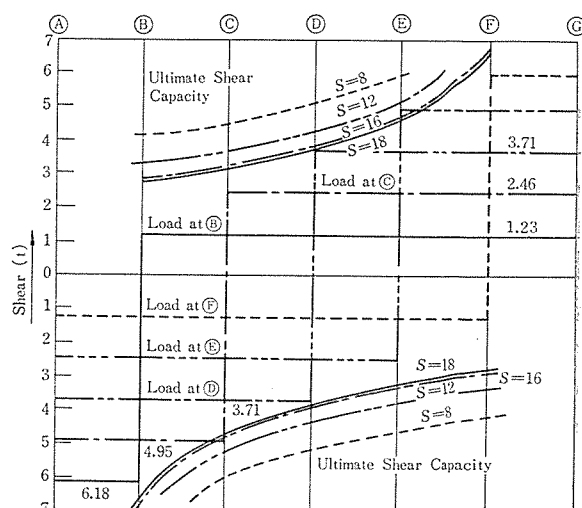
The flexural ultimate load acting at loading point D is obtained using the ultimate moment capacity  $M_u = 278 \times 10^3$  kg-cm.

$$P_u = \frac{4}{150} \times 278 \times 10^3 = 7.41 \text{ t}$$

Fig. 17 shows shear diagrams under the calculated ultimate load  $P_u$  acting at each loading point and the diagrams of the ultimate shear capacities of the sections.

Comparing these curves, it is clear that the ultimate shear capacities of the sections are

Fig. 17 Shear Diagrams & Shear Capacities



always greater than the shear produced by the load  $P_u$ , for the beams having the spacing of stirrups less than 12 cm. Flexural failures are expected for these beams. But the ultimate shear capacities are little less than the shear due to the load  $P_u$ , for the beams having the spacing of stirrups greater than 16 cm and shear failures are expected.

The test results are compared in Table 16 with the calculated values, with the exception of the beams No. 3 and No. 6 which clearly show the modes of failure due to ineffective anchorages of stirrups.

The test results on the beams with different amount of stirrups are clearly explained by the calculation applying the previous formulas.

## 4. Conclusions

For the range of beams tested, it appears that the ultimate shear capacity of a section can be

Table 16 Comparison between Calculated & Observed Values (F : Flexure, S : Shear)

Beam No.	(cm)	Calculated			Observed			Observed $V_u$
		Load Point	$V_u$ (t)	Mode of Failure	Load Point	$V_u$ (t)	Mode of Failure	
1	8	D	3.71	F	D	4.05	F	1.09
2	8	D	3.71	F	D	4.00	F	1.08
4	12	D	3.71	F	D	3.95	F	1.06
5*	16	D	3.71	F	D	4.02	F	1.08
7	18	C, E	4.62	S	C	4.90	S	1.06
8	18	C, E	4.62	S	E	4.76	S	1.03

\* For Beam No. 5 the calculated shear capacity of section C (or E) is almost equal to the shear due to  $P_u$  acting at this section. Therefore it is assumed in this Table that the flexural failure will be expected under load  $P_u$  acting at point D.

obtained by adding the shear producing an inclined crack to the shear carried by the web reinforcement.

The shear to produce an inclined crack, either web-shear or flexure-shear, can be estimated applying the formulas previously given in this paper.

The formula to evaluate the ultimate shear capacity of a section can also be applied to the beam subjected to a moving load and provided with several crosswise inclined cracks in its web due to the reversed action of shear. But the ultimate shear capacity of the beam subjected to a repeated moving load may be reduced by the existence of such crosswise inclined cracks in the web, because of their weakening the diagonal compressive struts in the cracked region.

The comparison between the calculated shear and the observed shear on the beams tested in the paper, shows a fairly good correlation between those two values.

Because of the limited tests reported here, the exact mechanism of shear failure still eludes authors grasp. The main stumbling block is the large number of interdependent parameters which influence the behaviour and mode of failure of a beam under bending and shear. To define design criteria which will satisfy the overall problem embracing all types of beams and all conditions of loading, the mechanism of shear failure should be more intensively investigated.

## 5. Acknowledgment

The author wishes to thank assistant professor

S. Kato and all other members of the Shibaura Institute of Technology who have assisted in this investigation.

## Reference

- 1) Rüschi, Vigerust : "Schubsicherung bei Spannbeton ohne Schubbewehrung", D.A.f.St. Heft 137 (1960)
- 2) Walter : "Über die Berechnung der Schubtragfähigkeit von Stahl- und Spannbetonbalken", Beton und Stahlbetonbau 11 (1962)
- 3) Bruce : "The action of vertical, inclined, and prestressed stirrups in prestressed concrete beams", PCI Journal February (1964)
- 4) Lorentsen : "Theory for the combined action of bending moment and shear in reinforced and prestressed concrete beams", ACI Journal April (1965)
- 5) Ojha : "The shear strength of rectangular reinforced and prestressed concrete beams", Magazine of Concrete Research No. 60 (1967)
- 6) Sheikh, Paiva : "Calculation of flexure-shear strength of prestressed concrete beams", PCI Journal February (1968)
- 7) Zwoyer, Siess : "Ultimate strength in shear of simply-supported prestressed concrete beams without web reinforcement", ACI Journal October (1954)
- 8) Hanson, Hulsbos : "Ultimate shear tests of prestressed concrete I-beams under concentrated and uniform loadings", PCI Journal June (1964)
- 9) MacGregor, Sozen, Siess : "Effect of draped reinforcement on behavior of prestressed concrete beams", ACI Journal December (1960)
- 10) Warner, Hall : "The shear strength of concrete beams without web reinforcement", Third Congress of the FIP (1958)
- 11) Evans, Hosny : "The shear strength of post-tensioned prestressed concrete beams", Third Congress of the FIP (1958)
- 12) Leonhardt : "Die verminderte Schubdeckung bei Stahlbeton Tragwerken", Der Bauingenieur Januar (1965)
- 13) MacGregor, Siess, Sozen : "Behavior of prestressed concrete beams under simulated moving loads", ACI Journal August (1966)

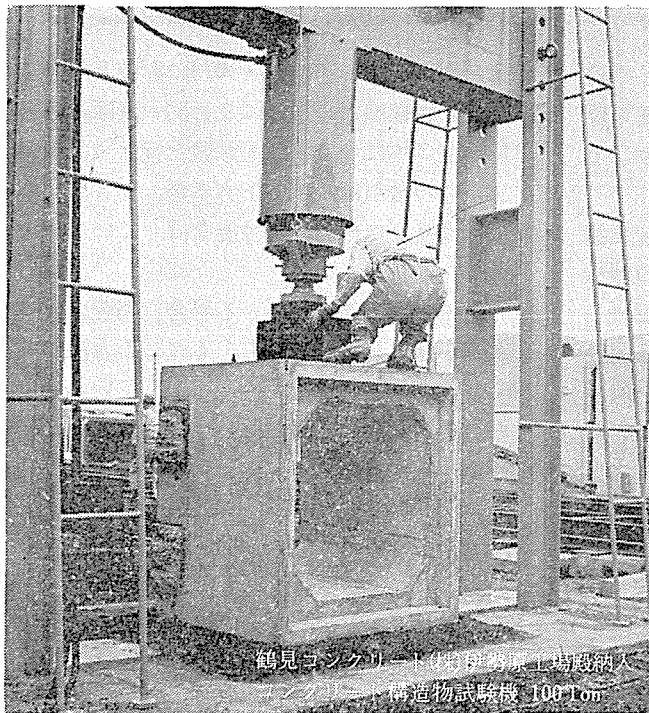
1969.8.4・受付

丸東リーレ式

# コンクリート構造物試験機

梁・カルバート・プレハブ材・プレキャスト製品など大型のコンクリート構造物の圧縮・曲げ試験がクローズ・アップされています。これらの試験機は、被試験供試体の形体に最も適した負荷部と、正確で操作の簡単な計測部との組み合わせが性能のきめ手となります。

当社のコンクリート構造物試験機は、ワンタッチ方式としてご好評を博している丸東リーレ式計測部を備え、多数の製作実績と共に必らずご満足頂ける試験機であります。



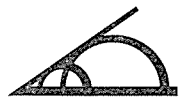
## 計測部の特長

- 1). 振子無交換式容量変換装置付  
容量変換 5段式
- 2). 容量と面盤の連動同時変換式
- 3). 過負荷防止装置付
- 4). 大型目盛盤(最小目盛1/500～1/600)付
- 5). オイル・バス式多連アクシアル・ポンプ付

## 負荷部の特長

- 1). 簡単かつ操作便利なフレーム構造
- 2). 加圧頭の高精度な平衡装置付

詳細資料をお送りいたします。  
誌名ご記入の上お申込下さい。



株式会社 丸東製作所

〒135-91  
コンクリート実験室  
京都出張所  
北海道出張所

東京都江東区深川白河町2-7 電話(03)642-5121(代)  
東京都江東区深川白河町2-9 電話(03)642-5121(代)  
京都市中京区壬生西土居の内町3-1 電話(311)7992  
札幌市南十条西十三丁目 電話(56)1409